Journal of Pharmacy

# Fabrication and Evaluation of Coaxial Core-Shell Electrospun *Curcuma xanthorrhiza* Nanofibres with Antibacterial Activity

Rafiqa Maisara Mohamad Rosly[1], Muhammad Taher[1*], Junaidi Khotib[2]

[1]*Department of Pharmaceutical Technology, Kulliyyah of Pharmacy, International Islamic University Malaysia, Jalan Sultan Ahmad Shah, 25200 Kuantan, Pahang, Malaysia.*
[2]*Faculty of Pharmacy, Universitas Airlangga, Surabaya, Indonesia*

## Abstract

**Introduction:** Chronic wounds are a major global health concern because their slow healing increases the risk of infection. Conventional dressings often fail to provide both effective antibacterial protection and optimal moisture control. Electrospun nanofibre membranes, with porous structures that resemble the extracellular matrix, offer a promising alternative. *Curcuma xanthorrhiza*, a traditional Southeast Asian rhizome, is rich in bioactive compounds such as curcumin and xanthorrhizol, which are known for their anti-inflammatory, antioxidant, and antibacterial properties. **Methods:** In this study, coaxial electrospinning was used to create core–shell nanofibre membranes, featuring polycaprolactone as the core and a gelatine/chitosan blend as the shell. *Curcuma* extract was incorporated at 1% (w/w) into the core. The resulting fibres were examined for their morphology, chemical composition, and thermal stability using scanning electron microscopy, Fourier transform infrared spectroscopy, and thermogravimetric analysis. Antibacterial activity was tested against *Staphylococcus aureus* and *Escherichia coli* using the disc diffusion method. **Results and Discussion:** Nanofibres loaded with *Curcuma* extract were smooth, continuous, and nanoscale in diameter, while fibres without extract were thicker due to a higher polymer concentration. The average fibre diameter ranged from 120.3 to 284.2 nm. Chemical analysis confirmed successful incorporation of the extract, with characteristic functional groups preserved and clear interactions between the polymers and bioactive compounds. Thermal analysis showed the fibres were stable up to 300°C. Antibacterial testing of *C. xanthorrhiza*-loaded nanofibres demonstrated no activity against *S. aureus* (0 mm) and *E. coli* (0 mm). **Conclusion:** In this study, *C. xanthorrhiza*-loaded nanofibres exhibit promising physical and chemical properties in their formulation. While the antibacterial activity was limited at the current tested concentration, it is suggested that the loading capacity of the extract be increased.

**Article history:**

Received: 1 April 2026
Accepted: 14 July 2026
Published: 31 July 2026

**Keywords:**

Polycaprolactone
Chitosan
Morphology
Electrospinning
Disk diffusion

doi: 10.31436/jop.v6i2.515

*Corresponding author's email: tahermuhammad@gmail.com

## Introduction

The skin is the largest organ in the body and acts as a crucial barrier to prevent microbiological, chemical, and physical harm. It triggers a natural healing process, but this process can be delayed in chronic or severe wounds, which leads to an elevated risk of infection. One to two percent of people worldwide, particularly in high-income countries, suffer from chronic wounds (Tamayo et al., 2022). China alone reported almost 30 million individuals with chronic wounds by 2022 (Zhang et al., 2022). Conventional dressings such as gauze are inert and non-occlusive, and their short-term antibacterial effectiveness is limited (Yu et al., 2019). Hydrogels are highly occlusive and retain large amounts of water, which may lead to wound maceration, especially in wounds with moderate to high exudate. On the other hand, nanofibre dressings provide a more balanced moisture environment while allowing vapor transmission due to their high porosity. Thus, many studies have nanofibre membranes that resemble the extracellular matrix (ECM), making them particularly applicable for use as wound dressings (Yang et al., 2020). Nanofibres have been produced using a variety of techniques, including electrospinning, drawing process, and template-assisted synthesis and self-assembly. However, electrospinning is becoming increasingly common because of its low cost, high yield, and incredible efficiency (Mouro & Gouveia, 2024; Komur et al., 2017). Electrospun nanofibres have been used successfully as wound dressings since 1977 (Liu et al., 2020). However, monoaxial electrospinning is hampered by difficulty in generating complex structures. To address such issues, coaxial electrospinning was developed. Coaxial electrospinning is preferred for wound healing because of its benefits, which include a simple manufacturing approach and a high drug-loading capacity (Ghazalian et al., 2022). In electrospinning, fibres are extracted from a polymer melt or solution using an electric field. A syringe pump, a collector connected to a grounded or negatively charged electric field, a spinneret attached to a positive electric field and high-voltage power are used in the setup (Zhao et al., 2024). In this study, Curcuma extract is encapsulated within nanofibre membranes using polycaprolactone (PCL) as the core and a gelatine/chitosan/(Gel/Ch) blend as the shell material. This approach is intended to provide a protective outer shell for the extract, prolong the release time, and enhance the mechanical properties of the nanofibre. The rhizome of *C. xanthorrhiza* contains a naturally occurring yellow polyphenolic compound called curcumin (Cur) (Petrai et al., 2025). It has been comprehensively studied due to its anti-inflammatory and antioxidant properties as well as its low toxicity (Pan et al., 2020). Additionally, Curcumin helps reduce the expression of pro-inflammatory cytokines such IL-6 and TNF-$\alpha$ (Wang et al., 2020). Furthermore, curcumin also promotes collagen deposition, cell migration and proliferation, all of which may accelerate the re-epithelialization of wounds in the late phases of the wound healing process (Rezaii et al., 2019). However, curcumin has limited use in wound healing because of its low bioavailability under physiological circumstances (Ratrey et al., 2020). Therefore, implementing *Curcuma* extract into the core layer of a coaxial delivery system can enhance its stability, achieve a continuous drug release pattern, and promote the skin regeneration process (Xia et al., 2022). The antimicrobial activity observed , which may be attributed to the presence of bioactive compounds in *C. xanthorrhiza* extract, including curcumin (Kocaadam & Şanlier, 2017).

A sesquiterpenoid known as xanthorrhizol has shown potent antibacterial effects against pathogens like *Bacillus cereus, Clostridium perfringens, Listeria monocytogenes,* and *Staphylococcus aureus* (Lee et al., 2008).

Electrospinning technology has advanced rapidly for developing novel wound dressings. However, most final product applications are still in the experimental stage and have not yet reached industrial production on a significant scale (Lu et al., 2024). Therefore, this study aims to fabricate and evaluate coaxial electrospun *C. xanthorrhiza*-loaded nanofibres and assess their physicochemical properties and antibacterial activity.

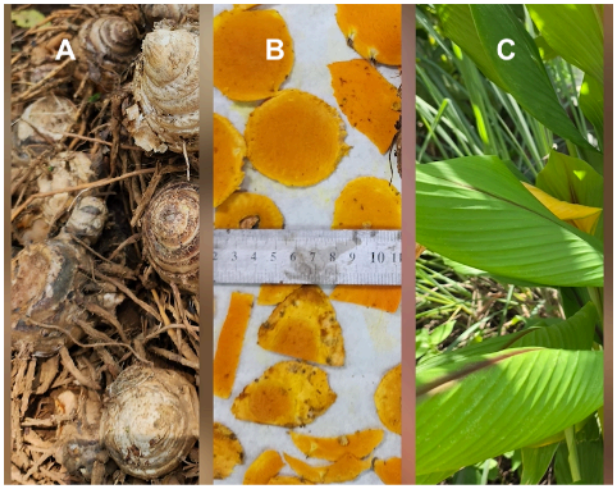


**Fig. 1**: Fresh rhizomes (A and B) and leaves of *C. xanthorrhiza* (C).

## Materials and methods

### *Materials*

Polycaprolactone (PCL; average Mn ~ 80,000) and chitosan were obtained from Sigma-Aldrich (Germany), while gelatine was also purchased from R&M Chemicals (Selangor, Malaysia). Glacial acetic acid and dimethyl sulfoxide (DMSO) were of analytical grade and used as received without further purification. *C. xanthorrhiza* Roxb. rhizomes were collected from Kuantan, Pahang, Malaysia, in September 2023. The voucher specimen (PIIUM 0379) is deposited at the Herbarium of the Kulliyyah of Pharmacy, the International Islamic University Malaysia. The rhizomes were cleaned, dried, and processed to obtain the crude extract, which was used for incorporation into nanofibre formulations and antibacterial testing. Solution preparation was carried out using a magnetic stirrer with temperature control. Sterilization of media and equipment was conducted using an autoclave operated at 121 °C for 15 minutes. Mueller–Hinton Agar (MHA) was obtained from Sigma-Aldrich (Germany). Sterile filter paper discs (6 mm diameter) were purchased commercially and used for the disc diffusion assay. Gentamycin discs (10 µg/disc) were used as the positive control for antibacterial evaluation. The bacterial strains *E. coli* (Gram-negative) and *S. aureus* (Gram-positive) were obtained from a recognised microbiology laboratory collection and maintained according to standard microbiological procedures.

### *Method*

#### *Extraction of Curcumin from Java turmeric Rhizomes (Curcuma xanthorrhiza)*

The extraction procedure began with freshly obtained *C. xanthorrhiza* (temulawak) rhizomes, which were chopped into small pieces using a chopper. The chopped rhizomes were weighed to obtain the required sample amount and then subjected to solvent extraction using an ethanol solution. The extraction was carried out using an ultrasonic bath at 60°C for 4 hours to facilitate the dissolution of xanthorrhizol, curcumin, and other bioactive compounds present in the rhizomes. After extraction, the mixture was allowed to cool to room temperature and was filtered to separate the liquid extract from the remaining plant residue. The filtrate was then concentrated using a rotary evaporator to remove excess solvent, forming a viscous ethanolic extract.

#### *Preparation of Electrospinning Solutions*

For the core solutions, a 20% (w/v) polycaprolactone (PCL) solution was prepared by dissolving 10 g of PCL in 50 mL of aqueous acetic acid for fibres without extract, while a 10% (w/v) PCL solution was prepared under the same conditions for fibres containing *C. xanthorrhiza* extract. The *Curcuma* extract was incorporated at 1% (w/w) relative to the polymer weight and stirred thoroughly until a uniform and homogeneous solution was obtained. For the shell solution, chitosan (5% w/v) and gelatine (30% w/v) were each dissolved separately in aqueous acetic acid and stirred until fully solubilized. The two polymer solutions were then combined in a 1:1 ratio to produce a homogeneous gelatine/chitosan (Gel/Ch) shell solution. All solutions were stirred continuously until clear and homogeneous coaxial electrospinning, ensuring optimal fibre formation and encapsulation of the bioactive extract.

#### *Coaxial Electrospinning Process*

For the preparation of core–shell nanofibres, the core solution consisted of PCL loaded with *Curcuma* extract, while the shell solution was composed of

gelatine and chitosan. Electrospinning was conducted using a Compact Electrospinning Unit (CES20, Nanolab Instruments Sdn Bhd, Malaysia) at an applied voltage of 12 kV, with a receiving distance of 15 cm between the needle tip and the collector. The flow rates of the core and shell solutions were set at 0.002 mL/min and 0.004 mL/min, respectively, under controlled humidity of 40–60% at room temperature. The process was continued for approximately 10 hours to obtain a uniform and stable nanofibre membrane (Xia et al., 2022). The resulting coaxial nanofibre membrane was then dried at room temperature to remove residual solvents and stored in a desiccator for further characterization and analysis.

*Morphological Characterization Using Scanning Electron Microscopy*

The morphology of the nanofibres was examined using a Carl Zeiss EVO MA10 scanning electron microscope (Carl Zeiss Microscopy GmbH, Germany). Before imaging, the samples were cut into small pieces, mounted on aluminium stubs, and sputter-coated with a thin layer of gold. Scanning electron microscopy (SEM) imaging was performed at an accelerating voltage of 10 kV (Hameed et al., 2022) and a working distance of 10.5 mm. Images were captured using a secondary electron detector (SE1) under high vacuum at 5,000× and 3000× magnification (Hameed et al., 2022).

*Chemical Characterization Using Fourier Transform Infrared Spectroscopy*

Fourier Transform Infrared Spectroscopy (FTIR) was performed using a Cary 630 FTIR spectrometer (Agilent Technologies, Inc., Santa Clara, CA, USA) to identify functional groups and analyse interactions between the *C. xanthorrhiza* extract and the polymeric matrix. Spectra were recorded over a range of 650–4000 $cm^{-1}$. The presence and positions of characteristic peaks were examined to confirm the incorporation of *Curcuma* extract and to detect any potential chemical bonding between the polymers and the bioactive compound. FTIR spectra of each pure component (*Curcuma* extract, PCL, gelatine, and chitosan) were recorded independently as references. By comparing the spectra of the pure materials with those of the composite nanofibres, the appearance, disappearance, or shifting of characteristic peaks was correlated to specific functional groups, thereby confirming molecular interactions and compatibility among the components.

*Thermal Stability Analysis Using Thermogravimetric Analysis*

The thermal stability and degradation behaviour of the nanofibres were analysed using a TG 309 Libra® thermogravimetric analyzer (NETZSCH- Gerätebau GmbH, Germany). The samples were heated from 25°C to 350°C at a constant heating rate of 15°C/min under a nitrogen atmosphere (Hameed et al., 2022). The obtained thermograms were used to determine the decomposition temperature and to assess the overall thermal stability of the electrospun nanofibre membranes.

*Antibacterial Activity Evaluation*

The antimicrobial activity of *Curcuma* extract was assessed against *E. coli* (Gram-negative) and *S. aureus* (Gram-positive) using the standard disc diffusion method (Tolun et al., 2025). The bacterial stock culture, which had been maintained on nutrient agar slants at 4 °C, was first revived by inoculating a single colony into nutrient broth and incubating at 37 °C for 18–24 h to obtain actively growing cells. The actively growing culture was then streaked onto fresh nutrient agar plates and incubated for an additional 18–24 h to isolate pure colonies and ensure culture viability. Subsequently, a single colony from the nutrient agar plate was transferred into Mueller–Hinton broth (MHB) and incubated at 37 °C for 18–24 h until the culture reached a turbidity equivalent to the 0.5 McFarland standard (*Performance Standards for Antimicrobial Disk Susceptibility Tests; Approved Standard — Eleventh Edition*, 2012). Mueller–Hinton Agar (MHA) was prepared according to the manufacturer's instructions and sterilized by autoclaving at 121 °C for 15 minutes. The molten agar was cooled to 45–50 °C and poured into sterile Petri dishes to form a uniform layer, which was allowed to solidify. Each plate was then inoculated by evenly spreading the standardised bacterial suspension using a sterile cotton swab. Sterile 5 mm fibre disc and 5 mm filter paper discs were

impregnated with 25 µL of *Curcuma* extract at three concentrations: 50 mg/mL, 100 mg/mL, and 200 mg/mL, corresponding to 1250 µg/disc, 2500 µg/disc, and 5000 µg/disc, respectively (Gupta et al., 2015). The impregnated discs were allowed to stand for 15 minutes to ensure proper diffusion of the extract and then aseptically placed onto the inoculated agar surface using sterile forceps. Gentamycin (10 µg/disc) was used as the positive control, while discs impregnated with DMSO served as the negative control. The plates were incubated at 37 °C for 12–14 hours (Gupta et al., 2015). All experiments were performed in triplicate (n = 3). After incubation, the diameter of the inhibition zones around each disc was measured in millimetres using a ruler. The presence of clear areas around the disc paper indicated antibacterial activity. The inhibition zone area was calculated by Equation 1 (Muchtaromah et al., 2020).

Inhibitory zone diameter = Clear zone diameter - Paper disc diameter (1)

## Results and discussion

*Extraction of Turmeric Rhizomes*

Extraction is an essential first step in isolating and purifying bioactive compounds from plant materials. The main goal of the extraction process is to obtain the highest possible yield with a high concentration of the desired active compounds. A well-controlled extraction process is therefore critical because it directly affects the quality, effectiveness, and reproducibility of the resulting extract. In this study, turmeric rhizomes were processed through several important stages, including collection, cleaning to remove dirt and impurities, drying to reduce moisture content, and solvent extraction. Each of these steps contributed to maintaining the stability of the bioactive compounds and improving extraction efficiency (Hashim & Bakar, 2024). Ultrasound-assisted extraction (UAE) is recognized as a successful extraction method that enhances yields and extract quality while reducing working durations. Using this method, 241.423 g of dried turmeric rhizome powder produced 36.733 g of oleoresin extract, giving an extraction yield of 15.21%. The application of these carefully controlled extraction conditions ensured the production of a high-quality oil extract, thereby supporting the consistency, reliability, and reproducibility of the subsequent experimental analyses. This yield closely resembles the results of previous studies using ultrasound-assisted extraction (UAE), which found that the oleoresin yields for *C. xanthorrhiza* and *C. domestica* were 15.66 ± 3.33% and 16.00 ± 4.67%, respectively (Nurhadi et al., 2020). The strong correlation between these results indicates that the extraction parameters used in this investigation were efficient and suitable, resulting in oleoresin yields that fell within the expected range. In comparison to previously published results for *C. xanthorrhiza* utilizing traditional extraction procedures, the extraction yield (15.21%) for this study is comparatively high. According to Mahadzir et al. (2025), Soxhlet extraction with ethanol typically yields 7.47–8.84%, , which indicates a lesser extraction efficiency and a longer processing time. Similarly, the oil yields obtained via Soxhlet extraction with hexane and percolation with ethanol were 5.88% and 11.73%, respectively (Salea et al., 2014), lower than the yield obtained in the present study. In short, UAE is a more effective extraction technique for xanthorrhizol and curcuminoid chemicals than other techniques (Rahmadansah et al., 2023). However, in the present study, the *C. xanthorrhiza* extract was not chemically standardised before incorporation into the electrospun nanofibres. The concentrations of curcumin, xanthorrhizol, and other bioactive constituents were not quantified using analytical techniques such as HPLC. Future investigations should include extract standardisation before formulation to ensure batch-to-batch consistency and facilitate correlation between bioactive compound concentration and biological activity.

*Morphology of Electrospun Nanofibres*

The electrospun 10% PCL fibres containing *Curcuma* extract exhibited a homogeneous, bead-free, and randomly oriented fibrous architecture with a narrower diameter distribution. The average fibre diameter was approximately 120.3 to 284.2 nm, confirming the formation of nanoscale fibres. The smooth surface morphology and absence of structural defects indicate a stable electrospinning jet. In contrast, the 20% PCL fibres without extract demonstrated substantially larger fibre diameters, ranging from 374 nm to 857 nm, with a broader size distribution. Although the fibres remain continuous and free from bead formation, the increased diameter can be attributed to the elevated polymer concentration, which significantly increases solution viscosity and polymer chain entanglement. High viscosity restricts jet thinning during electrospinning, leading to reduced stretching and the deposition of thicker fibres on the collector (Gürtler et al., 2024). Feng et al. (2025) demonstrated that raising the PCL concentration to 22.41 wt.% prevented the formation of beads but produced larger fibres because excessive viscoelastic resistance made it difficult for the jet to effectively attenuate, thereby producing thicker fibres with a lower specific surface area. Similarly, Mochane et al., 2019 found that at 17 wt.% PCL, fibres with a diameter of ~211 nm were accompanied by large beads (~15 μm), but at 19 wt.%, continuous fibres without beads were formed. However, thick microfibres were produced as a result of increased solution viscosity when PCL concentration exceeded 19 wt.% demonstrating that excessive polymer concentration hurt fibre refinement. Wenchao et al. (2017) examined the electrospinning of PCL nanofibres utilising water ($H_2O$) as an additive in a solution of PCL and glacial acetic acid. While water ($H_2O$) was not utilised as a solvent for PCL electrospinning in this investigation, it was used to ionize acetic acid and boost conductivity. This work involved dissolving PCL in glacial acetic acid to get 17–23% PCL, which is consistent with these studies. The incorporation of *Curcuma* extract is expected to increase the solution conductivity and solid content due to the presence of phytoconstituents, thereby enhancing electrostatic stretching forces acting on the polymer jet (Hameed et al., 2022). The concentration of *Curcuma* extract used in this study was fixed at 1%, which is close to the lower boundary of the optimal range (1.2–2.4%) reported in the literature for electrospun PCL-based systems. Previous studies have demonstrated that curcuma concentrations within this range provide a favourable balance between fibre morphology, mechanical performance, and biological response (Yoshikawa et al., 2025). Therefore, the selection of 1% curcuma extract represents a conservative yet effective concentration that ensures stable electrospinning and desirable nanofibre morphology while remaining consistent with the previously reported optimal *curcuma* loading range. One limitation of this study is that statistical analysis of the fibre diameter distribution was not performed. Although representative fibre diameters were obtained from SEM images to characterise the morphology of the electrospun membranes, statistical comparison between different formulations could not be established. Future studies should include quantitative fibre diameter analysis from a larger number of measurements followed by appropriate statistical analyses, such as analysis of variance (ANOVA), to provide more robust comparisons of fibre morphology and fabrication reproducibility.

*FTIR Characterization of PCL, Chitosan, Gelatine, Curcuma, and GEL/CS/Curcuma/PCL Composite Fibre*

The FTIR spectra of the individual components—PCL, chitosan, gelatine, and *C. xanthorriza*—confirmed the presence of characteristic functional groups and the chemical integrity of each material. The PCL nanofibres exhibited a prominent peak at 1720.2 $cm^{-1}$, corresponding to ester carbonyl (C=O) stretching, along with methylene ($–CH_2$) stretching

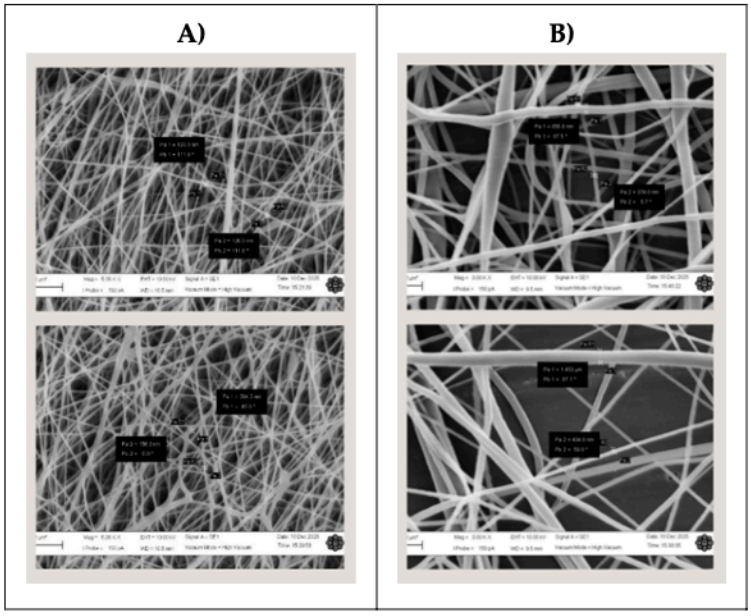


**Fig. 2**: SEM images showing the morphological characteristics of A) 10% PCL nanofibres incorporated with extract, and B) electrospun 20 % PCL nanofibres without extract.

bands at 2940.9 $cm^{-1}$ and 2864.5 $cm^{-1}$, and a C–O–C stretching vibration at 1159.2 $cm^{-1}$, consistent with previous reports and indicative of the polymer backbone and amorphous phase (Ali et al., 2014; Caglayan & Basal, 2020; Wang et al., 2023). Chitosan nanofibres showed a broad O–H and N–H stretching band at 3356.5 $cm^{-1}$, and characteristic amide I and II peaks at 1653.1 $cm^{-1}$ and 1576.7 $cm^{-1}$, confirming the presence of N-acetylated residues and hydrogen bonding, while the peak at 1023.2 $cm^{-1}$ represented C–O stretching of the polysaccharide backbone (Chen et al., 2011; Teanchai et al., 2016; Wang et al., 2004; Yasmeen et al., 2016). Gelatine exhibited protein-associated bands, with O–H and N–H stretching at 3272.6 $cm^{-1}$ (Amide A), C=O stretching at 1623.3 $cm^{-1}$ (Amide I), N–H bending and C–N stretching at 1522.6 $cm^{-1}$ (Amide II), and C–N stretching with N–H in-plane bending at 1235.6 $cm^{-1}$ (Amide III), reflecting its polypeptide backbone and secondary structure (Das et al., 2017; Hassan et al., 2021; Pradini et al., 2018). The *C xanthorriza* extract displayed a broad O–H stretching band at 3280.1 $cm^{-1}$, aromatic C=C stretching at 1591.6 $cm^{-1}$, and C–O stretching at 1023.2 $cm^{-1}$, confirming the presence of phenolic and curcuminoid functional groups and hydrogen-bonded hydroxyls (Kusumadewi et al., 2022). These FTIR results confirmed that all materials retained their characteristic chemical structures, which is essential for their subsequent use in composite nanofibre fabrication.

Meanwhile, the FTIR spectrum of the GEL/CS/*Curcuma*/PCL composite fibre revealed distinct peaks corresponding to the characteristic functional groups of its individual components, confirming successful incorporation and interactions within the fibre matrix. The peaks at ~2939 $cm^{-1}$ and ~1720.2 $cm^{-1}$ were assigned to asymmetric $CH_2$ stretching and ester carbonyl (C=O) stretching of PCL, respectively. These values align well with previous reports, where PCL shows $CH_2$ stretching around 2944 $cm^{-1}$ and C=O stretching near 1727 $cm^{-1}$, indicating that the polymer backbone remained intact during fibre fabrication (Ghaee et al., 2019). Curcumin-related peaks were observed at approximately 3527.9 $cm^{-1}$ and 1636.3 $cm^{-1}$, corresponding to O–H stretching and aromatic C=C stretching, respectively. These findings are consistent with the literature, where curcumin-loaded composites exhibit C=C stretching vibrations of the benzene rings around 1650, 1628, 1625, and 1616 $cm^{-1}$ and phenolic O–H stretching near 3513 $cm^{-1}$ (Chiaoprakobkij et al., 2020). This confirms that *curcuma* extract was successfully incorporated into the fibre and retained its

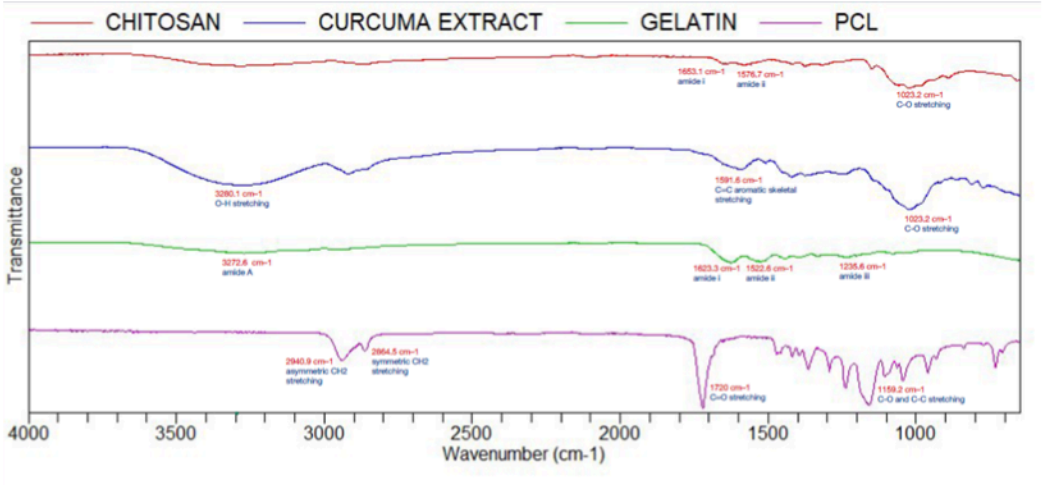


**Fig. 3:** FTIR spectra of individual compounds: curcuma, PCL, gelatine, and chitosan.

functional groups after processing. The contribution of chitosan and gelatine to the composite structure was evident from the peaks at 1636.3, 1470.4, and 1239.3 $cm^{-1}$, corresponding to amide I, amide II/CH bending, and amide III, respectively. Compared to the spectra of the individual polymers, these shifts indicate the formation of hydrogen bonds and electrostatic interactions between the amino groups of chitosan and the carbonyl groups of gelatine, consistent with previous studies on GEL/CS composites (Momtaz et al., 2024). The slight shifts in amide I and II peaks reflect these polymer-polymer interactions, while the presence of curcuma and PCL contributes additional O–H groups and hydrophobic interactions.

*Thermal Stability and Decomposition of Nanofibres*

The thermogravimetric analysis (TGA) curve shows that the PCL–Curcuma extract electrospun nanofibres are thermally stable up to approximately 300 °C, with very little weight loss at lower temperatures. This minimal early weight loss indicates that there is no significant residual solvent or moisture, confirming effective solvent evaporation during the electrospinning process (Rêgo et al., 2025). Previous studies report that the main stage of thermal decomposition occurred at higher temperatures (350–600 °C), characterized by significant weight loss due to the degradation of the polymer backbone and other complex organic structures (Koochaki et al., 2025). The onset of the significant weight loss in the TGA curve around ~300–350 °C, with a distinct peak in the DTG at ~320–325 °C, corresponds closely to the main decomposition of the PCL polymer backbone, a behaviour commonly reported in the literature where PCL shows a single major degradation step in this temperature range (Ismail & Ahmad Shariff, 2021). Curcumin, the active compound in turmeric (*Curcuma*), shows no weight loss up to approximately 190 °C, and a decomposition peak at 292 °C, with significant degradation occurring beyond this temperature (Chen et al., 2014). This suggests that *C. xanthorrhiza*, which contains similar compounds, may exhibit a comparable thermal stability profile. In our study, the decomposition of *curcuma* extract is not visible. The decomposition of *curcuma* may be masked by the predominant degradation of the PCL matrix in TGA thermograms (Pompa-Monroy et al., 2020). The impact of curcuma extract on the thermal stability of PCL after electrospinning has been explored in several studies. *Curcuma* incorporation into PCL fibres do not significantly affect the decomposition of PCL. This was demonstrated in a study that investigated the effect of curcumin on the thermal stability and degradation behaviour of PCL and its blend with poly (glycolic acid) (PGA) using TGA. The results showed that the incorporation of curcuma had only a minimal effect on the thermal stability of PCL, while it significantly influenced the degradation behaviour of PGA (Sleinus et al., 2025).

*Antimicrobial Activity of Electrospun Nanofibres Using the Disk Diffusion Method*

The antimicrobial activity of *C. xanthorrhiza* has been studied using several disease-causing microbes. The tested pathogens were *S. mutans*, *S. aureus*, *E. coli*, and *B. cereus*. could cause serious diseases such as foodborne illness, dental plaque, skin disease, infectious disease, pneumonia, tuberculosis, pulp necrosis, diarrhoea, typhus, acne, nosocomial infections, hospital-acquired infections, filamentous fungal infections, nail infection, and penicilliosis (Akhtar et al., 2021). The antimicrobial activity of *C. xanthorrhiza* is largely attributed to its rich content of

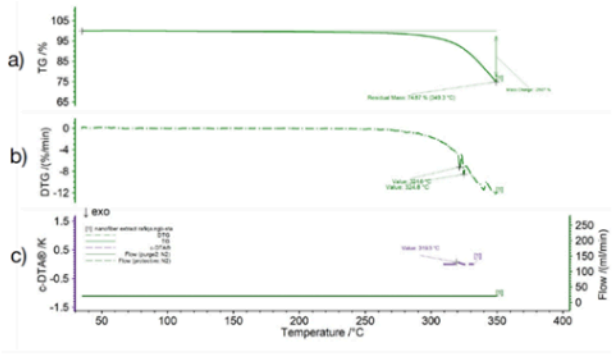


**Fig. 4:** Thermal analysis of 10% electrospun nanofibres loaded with Curcuma extract: (a) TGA curve (% weight loss vs. temperature), (b) DTG curve (derivative weight (%/min) vs. temperature), (c) cDTA curve (heat flow vs. temperature)

phenolic compounds, particularly xanthorrhizol and curcuminoids, which are considered the major bioactive constituents. Phenolic compounds are known to exert antimicrobial effects by disrupting microbial cell walls and membranes, leading to increased membrane permeability and subsequent leakage of essential intracellular components such as ATP, RNA, proteins, and DNA. This loss of vital molecules ultimately interferes with cellular metabolism and compromises microbial survival (Akhtar et al., 2021). Although the precise antimicrobial mechanism of xanthorrhizol has not been fully elucidated, it has been suggested that xanthorrhizol may suppress key intracellular signaling pathways, including nuclear factor kappa B (NF-κB) and mitogen-activated protein kinase (MAPK), which are activated during microbial infection. Such inhibition may contribute to the reduced viability and proliferation of microbial cells. Curcumin, which is another principal compound in *C. xanthorrhiza*, exhibits antimicrobial activity through multiple mechanisms. It has been reported to inhibit cytokinesis and bacterial cell multiplication by interfering with cell division processes, as well as by disrupting the integrity of bacterial cell walls and membranes, leading to cell lysis (Akhtar et al., 2021). The antibacterial effects of r *C. xanthorrhiza* extract against Staphylococcus have also been associated with the presence of various secondary metabolites, including essential oils, curcumin, alkaloids, flavonoids, terpenoids, phenols, and tannins (Dermawaty, 2015). Among these, curcumin and xanthorrhizol demonstrate broad-spectrum antibacterial activity against both Gram-positive and certain Gram-negative bacteria. However, their effects are generally more pronounced against Gram-positive bacteria, likely due to differences in cell wall composition. Curcumin also exhibits phototoxic effects, where exposure to light induces the production of hydrogen peroxide, causing oxidative damage to bacterial cytoplasmic membranes (Warmasari et al., 2020). Additionally, Akarchariya et al. (2017) also observed that antimicrobial activity may be attributed to the presence of monoterpenes and sesquiterpenes as the major constituents, particularly oxygenated monoterpenes such as camphor and 1,8-cineole, as well as sesquiterpenes like germacrene, which have previously been reported to exhibit strong antibacterial properties. The antibacterial activity of temulawak rhizome extract was evaluated against *S. aureus and E. coli*, and the results are summarised in Table 1.

**Table 1:** Inhibition zone of *Curcuma* extract against *S. aureus* and *E. coli* at varying concentrations.

| Concentration of Extract (mg/ml) | S. aureus (mm) Mean ± SD | E. coli (mm) Mean ± SD |
|---|---|---|
| 200 | 8.7 ± 0.58 | 1.7 ± 0.58 |
| 100 | 7.7 ± 0.58 | 1.3 ± 0.58 |
| 50 | 7.7 ± 0.58 | 1.0 ± 0.00 |

*The inhibition zone of gentamycin was 20.0 mm against S. aureus and 14.0 mm against E. coli.

All three extract treatments for *S. aureus* exhibited weak antibacterial activity, with mean inhibition zone diameters of 8.7, 7.7, and 7.7 mm for 50, 100, and 200 mg/mL, respectively. In contrast to earlier findings that used different solvent fractions, the methanolic fraction had greater activity against *S. aureus* (12–22 mm) at the same doses (50, 100, and 200 mg/mL) (Gupta et al., 2015). The ethanolic extract demonstrated much lower antibacterial activity when evaluated at the same concentrations, indicating that the antibacterial activity may be enhanced by the extraction process, component concentration, or particular phytochemicals extracted in methanol. No inhibition was observed in the negative control (DMSO), confirming the validity of the assay. These results indicate that while the *Curcuma* extract can inhibit *S. aureus* growth, its antibacterial effect is considerably weaker than that of the standard antibiotic. In the case of *E. coli*, the extract showed very limited activity, with inhibition zone diameters of 1.7, 1.3, and 1.0 mm, all categorized as weak according to (Ponce et al., 2003). Ponce et al. categorised antibacterial activity into four levels based on the diameter of the inhibition zone, namely weak (not sensitive), moderate (sensitive), strong (very

sensitive), and very strong (extremely sensitive). According to this classification, antibacterial activity is considered weak when the inhibition zone diameter is less than 8 mm, moderate when it ranges from 8 to 14 mm, strong when it falls between 15 and 19 mm, and very strong when the inhibition zone exceeds 20 mm. Gentamycin, used as a positive control, produced a significantly larger inhibition a zone of 13 mm, while no inhibition was observed in the negative control. These findings confirm that Gram-negative bacteria are less susceptible to *Curcuma* rhizome extract, likely due to the presence of an outer membrane that limits the penetration of bioactive compounds (Hashim & Bakar, 2024). The effectiveness of antibacterial agents can be influenced by several factors, such as the concentration of the substance, the number of active compounds it contains, the number of microorganisms present, and environmental conditions like temperature and pH. In this study, not only the concentration but also the bioactive compound content in the temulawak rhizome extract appeared to play an important role in its antibacterial activity (Warmasari et al., 2020). The temulawak (*C. xanthorrhiza* Roxb.) rhizome extract demonstrated antibacterial activity, but its efficacy was lower than that of gentamycin, the positive control. This difference likely reflects the lower concentration of active antibacterial compounds in the extract and its dose-dependent activity. Furthermore, the mode of action may differ between the two agents: gentamycin acts bactericidally, directly killing bacteria, whereas temulawak extract appears to be bacteriostatic, inhibiting bacterial growth without inducing cell death (Warmasari et al., 2020; Tsao et al., 2021). The solvent, which is DMSO, was reported to have no antibacterial activity against Gram-positive and Gram-negative bacteria, which did not affect the results of the study (Prijatmoko et al., 2018).

Unlike the free *C. xanthorrhiza* extract, which exhibited weak antibacterial activity against *S. aureus* and *E. coli*, the electrospun nanofibres containing 1% extract did not produce measurable inhibition zones. Similar electrospun wound dressing systems (Arampatzis et al., 2021) incorporating natural bioactive compounds have generally demonstrated improved antibacterial performance when higher concentrations of the active compound were added. In the present study, the absence of inhibition zones may be attributed to the relatively low extract loading (1%), together with encapsulation of the extract within the PCL core, which may have restricted the diffusion of antibacterial compounds into the agar medium during the disc diffusion assay. Therefore, although the coaxial architecture provides protection for sensitive phytochemicals and offers potential for sustained drug release, optimisation of extract loading, release kinetics, and fibre composition is required to enhance antibacterial efficacy.

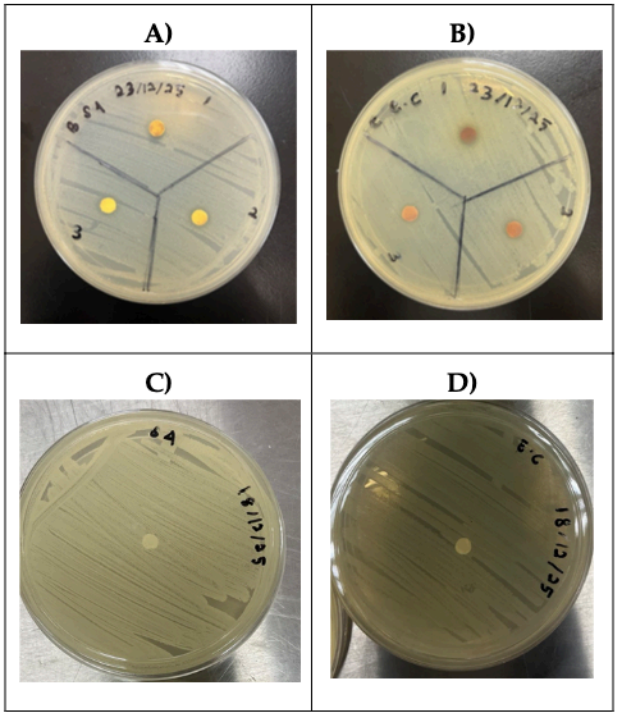


**Fig. 5:** Inhibition zones produced by (A) Curcuma extract against *S. aureus*, (B) Curcuma extract against *E. coli*, (C) Curcuma extract-loaded nanofibres against S. aureus, (D) Curcuma extract-loaded nanofibres against E. coli

## Conclusion

In this study, coaxial electrospinning was successfully employed to fabricate core–shell nanofibrous membranes composed of PCL and a gelatine/chitosan (Gel/Ch) blend, with *C. xanthorrhiza* extract incorporated as a natural antibacterial agent. The produced nanofibres exhibited uniform, bead-free morphology with smooth surfaces and nanoscale diameters, indicating stable jet formation and effective encapsulation of the extract. FTIR analysis confirmed good chemical compatibility among the polymer components and the incorporated extract, while TGA demonstrated that the nanofibres remained thermally stable up to approximately 300

°C, suggesting that the addition of *Curcuma* extract did not adversely affect the intrinsic thermal stability of PCL. Antibacterial evaluation showed that the Curcuma extract possessed weak inhibitory activity, with greater effectiveness against *S. aureus* than *E. coli*. However, at a loading concentration of 1% (w/v), the electrospun nanofibrous membranes did not exhibit observable inhibition zones, indicating that this concentration was insufficient to achieve significant antibacterial performance. These results suggest that further optimisation of extract loading, fibre architecture, and release characteristics is necessary to enhance the antibacterial efficacy of the nanofibrous system.

## Authors contributions

Conceptualization, Supervision, validation, writing—review and editing: MT and J.K; methodology, formal analysis, investigation, data curation, writing—original draft preparation: RMMR

## Acknowledgements

The authors would like to express their sincere appreciation to the International Islamic University Malaysia for the research facility.

## Conflict of interest

The authors declare no conflict of interest.

## Declaration of generative AI and AI-assisted technologies in the writing process

During the preparation of this work, the authors used ChatGPT to assist in improving language clarity and readability. After using this tool, the authors carefully reviewed, edited, and revised the content as necessary and take full responsibility for the final content of the publication.

## References

Akarchariya, N., Sirilun, S., Julsrigival, J., & Chansakaowa, S. (2017). Chemical profiling and antimicrobial activity of essential oil from *Curcuma aeruginosa* Roxb., *Curcuma glans* K. Larsen & J. Mood and *Curcuma cf. xanthorrhiza* Roxb. collected in Thailand. *Asian Pacific Journal of Tropical Biomedicine*, *7*(10), 881–885. https://doi.org/10.1016/j.apjtb.2017.09.009

Akhtar, N., Wani, A. K., Mir, T.U.G., Kumar, N., & Mannan, M.A.U. (2021). Ethnomedicinal uses, phytochemistry, and pharmacological activities. *Plant Cell Biotechnology and Molecular Biology*. 22 (41-42), 300–319

Ali, S., Khatri, Z., Oh, K. W., Kim, I., & Kim, S. H. (2014). Preparation and Characterization of Hybrid Polycaprolactone / Cellulose Ultrafine Fibres via Electrospinning. *Macromolecular Research*, *22*(5), 562–568. https://doi.org/10.1007/s13233-014-2078-x

Arampatzis, A. S., Kontogiannopoulos, K. N., Theodoridis, K., Aggelidou, E., Rat, A., Willems, A., Tsivintzelis, I., Papageorgiou, V. P., Kritis, A., & Assimopoulou, A. N. (2021). Electrospun wound dressings containing bioactive natural products: Physico-chemical characterization and biological assessment. *Biomaterials Research*, *25*(1), 23. https://doi.org/10.1186/s40824-021-00223-9

Caglayan, B., & Basal, G. (2020). Electrospun Polycaprolactone / Silk Fibroin Nanofibres Loaded with Curcumin for Wound Dressing Applications. Digest Journal of Nanomaterials and Biostructures. 15(4), 1165–1173.

Chen, G., Mi, J., Wu, X., Luo, C., Li, J., Tang, Y., & Li, J. (2011). Structural features and bioactivities of the chitosan. *International Journal of Biological Macromolecules*, *49*(4), 543–547. https://doi.org/10.1016/j.ijbiomac.2011.06.009

Chen, Z., Xia, Y., Liao, S., Huang, Y., Li, Y., He, Y., Tong, Z., & Li, B. (2014). Thermal degradation kinetics study of curcumin with nonlinear methods. *Food Chemistry*, *155*, 81–86. https://doi.org/10.1016/j.foodchem.2014.01.034

Chiaoprakobkij, N., Suwanmajo, T., Sanchavanakit, N., & Phisalaphong, M. (2020). Curcumin-Loaded Bacterial Cellulose/Alginate/Gelatin as A Multifunctional Biopolymer Composite

Film. *Molecules*, *25*(17), 3800. https://doi.org/10.3390/molecules25173800

Dermawaty, D. E. (2015). Potential extract curcuma (*Curcuma xanthorriza* , Roxb ) as antibacterials. *Jurnal Majority*, *4*(1), 5–11.

Das, M. P., Suguna, P. R., Prasad, K., Vijaylakshmi, J. V, & Renuka, M. (2017). Extraction and Characterization of Gelatine: A Functional Biopolymer. *International Journal of Pharmacy and Pharmaceutical Sciences*. *9*(9), 4–7. hhttps://doi: 10.22159/ijpps.2017v9i9.17618

Feng, D., Li, Y., Zheng, Y., Chen, J., Zhang, X., Li, K., Shen, J., & Guo, X. (2025). Study on the Electrospinning Fabrication of PCL/CNTs Fiber Membranes and Their Oil–Water Separation Performance. *Polymers*, *17*(12), 1705. https://doi.org/10.3390/polym17121705

Ghaee, A., Bagheri-Khoulenjani, S., Afshar, H., & Bogheiri, H. (2019). Biomimetic nanocomposite scaffolds based on surface modified PCL-nanofibres containing curcumin embedded in chitosan/gelatine for skin regeneration. *Composites Part B: Engineering*, *177*, 107339. https://doi.org/10.1016/j.compositesb.2019.107339

Ghazalian, M., Afshar, S., Rostami, A., Rashedi, S., & Bahrami, S. H. (2022). Fabrication and characterization of chitosan-polycaprolactone core-shell nanofibres containing tetracycline hydrochloride. *Colloids and Surfaces A: Physicochemical and Engineering Aspects*, *636*, 128163. https://doi.org/10.1016/J.COLSURFA.2021.128163

Gupta, A., Mahajan, S., & Sharma, R. (2015). Evaluation of antimicrobial activity of Curcuma longa rhizome extract against Staphylococcus aureus. *Biotechnology Reports*, *6*, 51–55. https://doi.org/10.1016/j.btre.2015.02.001

Gürtler, A. L., Linseisen, I., Grohganz, H., & Heinz, A. (2024). Coaxial electrospinning of polycaprolactone – A design of experiments approach. *European Polymer Journal*, *208*(February), 112886. https://doi.org/10.1016/j.eurpolymj.2024.112886

Hameed, A., Rehman, T. U., Rehan, Z. A., Noreen, R., Iqbal, S., Batool, S., Qayyum, M. A., Ahmed, T., & Farooq, T. (2022). Development of polymeric nanofibres blended with extract of neem (*Azadirachta indica*), for potential biomedical applications. *Frontiers in Materials*, *9*(November), 1–10. https://doi.org/10.3389/fmats.2022.1042304

Hassan, N., Ahmad, T., Zain, N. M., & Awang, S. R. (2021). Identification of bovine, porcine and fish gelatin signatures using chemometrics fuzzy graph method. *Scientific Reports*, *11*(1), 9793. https://doi.org/10.1038/s41598-021-89358-2

Kocaadam, B., & Şanlier, N. (2017). Curcumin, an active component of turmeric (Curcuma longa), and its effects on health. *Critical Reviews in Food Science and Nutrition*, *57*(13), 2889–2895. https://doi.org/10.1080/10408398.2015.1077195

Komur, B., Bayrak, F., Ekren, N., Eroglu, M. S., Oktar, F. N., Sinirlioglu, Z. A., Yucel, S., Guler, O., & Gunduz, O. (2017). Starch/PCL composite nanofibres by co-axial electrospinning technique for biomedical applications. *BioMedical Engineering OnLine*, *16*(1), 40. https://doi.org/10.1186/s12938-017-0334-y

Koochaki, S., Arabshahi-Delouee, S., Sheikh Arabi, M., Fadavi, A., & Ardebili, A. (2025). Innovation in sustainable packaging for red meat: Electrospun polycaprolactone nanofibres with purslane (*Portulaca oleracea* L.) extract and oil. *LWT*, *231*(August). https://doi.org/10.1016/j.lwt.2025.118294

Kusumadewi, A. P., Martien, R., Pramono, S., Setyawan, A. A., Windarsih, A., Rohman, A., Kusumadewi, A. P., Martien, R., Pramono, S., Anita, A., Setyawan, A., & Windarsih, A. (2022). Application of FTIR spectroscopy and chemometrics for correlation of antioxidant activities, phenolics and flavonoid contents of

Indonesian *Curcuma xanthorrhiza*. *International Journal of Food Properties*, *25*(1), 2364–2372. https://doi.org/10.1080/10942912.2022.2134418

Lee, L. E. E. Y., Shim, J., & Rukayadi, Y. (2008). Antibacterial Activity of Xanthorrhizol Isolated from *Curcuma xanthorrhiza* Roxb. against Foodborne Pathogens. *Journal of Food Protection*, *71*(9), 1926–1930. https://doi.org/10.4315/0362-028X-71.9.1926

Liu, Z., Ramakrishna, S., & Liu, X. (2020). Electrospinning and emerging healthcare and medicine possibilities. *APL Bioengineering*, *4*(3), 30901. https://doi.org/10.1063/5.0012309

Lu, X., Zhou, L., & Song, W. (2024). Recent Progress of Electrospun Nanofibre Dressing in the Promotion of Wound Healing. *Polymers*, *16*(18). https://doi.org/10.3390/POLYM16182596

Mahadzir, M. M., Azira, N., & Muhammad, I. (2025). Antioxidant Potential of *Curcuma xanthorrhiza* -based Serum Stick. *Scientific Research Journal*, *22*(1), 83–100.

Mochane, M. J., Motsoeneng, T. S., Sadiku, E. R., Mokhena, T. C., & Sefadi, J. S. (2019). Morphology and Properties of Electrospun PCL and Its Composites for Medical Applications: A Mini Review. *Applied Sciences*, *9*(11), 2205. https://doi.org/10.3390/app9112205

Momtaz, M., Momtaz, E., Mehrgardi, M. A., Momtaz, F., Narimani, T., & Poursina, F. (2024). Preparation and characterization of gelatine / chitosan nanocomposite reinforced by NiO nanoparticles as an active food packaging. *Scientific Reports*, 1–11. https://doi.org/10.1038/s41598-023-50260-8

Mouro, C., & Gouveia, I. C. (2024). Electrospun wound dressings with antibacterial function: a critical review of plant extract and essential oil incorporation. *Critical Reviews in Biotechnology*, *44*(4), 641–659. https://doi.org/10.1080/07388551.2023.2193859

Muchtaromah, B., Savitri, E., Fitriasari, P., & Istiwandhani, J. (2020). Antibacterial activities of *Curcuma mangga* Val. extract in some solvents to *Staphylococcus aureus* and *Escherichia coli*. *AIP Conference Proceedings*. 2231. https://doi.org/10.1063/5.0002490

Nurhadi, B., Saputra, R., Setiawati, T., Husein, S., Faressi, F., Utari, C., Sukri, N., Kayaputri, I., & Setiasih, I. (2020). Comparison of *Curcuma domestica* and *Curcuma xanthorrhiza* oleoresins extracted using maceration, Soxhlet, and ultrasound-assisted extraction (UAE). *IOP Conference Series: Earth and Environmental Science*, *443*, 12074. https://doi.org/10.1088/1755-1315/443/1/012074

Pan, H., Shen, X., Tao, W., Chen, S., & Ye, X. (2020). Fabrication of Polydopamine-Based Curcumin Nanoparticles for Chemical Stability and pH-Responsive Delivery. *Journal of Agricultural and Food Chemistry*, *68*(9), 2795–2802. https://doi.org/10.1021/acs.jafc.9b07697

*Performance Standards for Antimicrobial Disk Susceptibility Tests; Approved Standard — Eleventh Edition* (Vol. 32, Issue 1). (2012).

Petrai, N., Loukelis, K., & Chatzinikolaidou, M. (2025). Curcumin-Functionalized Electrospun Nanofibrous Membranes with Antimicrobial Activity for Wound Healing. *Nanomaterials*, *15*(5). https://doi.org/10.3390/nano15050388

Pompa-Monroy, D. A., Figueroa-Marchant, P. G., Dastager, S. G., Thorat, M. N., Iglesias, A. L., Miranda-Soto, V., Pérez-González, G. L., & Villarreal-Gómez, L. J. (2020). Bacterial biofilm formation using pcl/curcumin electrospun fibres and its potential use for biotechnological applications. *Materials*, *13*(23), 1–22. https://doi.org/10.3390/ma13235556

Ponce, A. G., Fritz, R., Valle, C. E., & Roura, S. I. (2003). Antimicrobial activity of essential oils on native microbial population of organic Swiss Chard. *LWT - Food Science and Technology*, *36*, 679–684. https://doi.org/10.1016/S0023-6438(03)00088-4

Pradini, D., Juwono, H., Anoraga, K., & Kurniawan, F. (2018). *A preliminary study of identification halal gelatine using quartz crystal microbalance (QCM) sensor*. Malaysian Journal of Fundamental and Applied Sciences. *14*(3), 325–330.

Prijatmoko, D., Syafira, N. L., & Lestari, P. E. (2018). Antibacterial activity of essential oil extracts from Curcuma xanthorrhiza roxb. rhizomes against bacteria causing pulp necrosis. *Journal of Dentomaxillofacial Science*, *3*(3), 144. https://doi.org/10.15562/jdmfs.v3i3.763

Rahmadansah, R., Rahayu, D. S., & Raisyadikara, F. (2023). Meta-analysis on extraction methods, pharmacological activities, and cultivation techniques of *Curcuma xanthorrhiza* Roxb. *Indonesian Journal of Agronomy*. 51, 163–172.

Ratrey, P., Dalvi, S. V, & Mishra, A. (2020). Enhancing Aqueous Solubility and Antibacterial Activity of Curcumin by Complexing with Cell-Penetrating Octaarginine. *ACS Omega*, *5*(30), 19004–19013. https://doi.org/10.1021/acsomega.0c02321

Rêgo, T. R. S., Toledo, A. L. M. M., & Dias, M. L. (2025). Effect of Processing on the Morphology and Structure of PLGA/PVA Fibres Produced by Coaxial Electrospinning. *Processes*, *13*(6). https://doi.org/10.3390/pr13061837

Rezaii, M., Oryan, S., & Javeri, A. (2019). Curcumin nanoparticles incorporated collagen-chitosan scaffold promotes cutaneous wound healing through regulation of TGF-β1/Smad7 gene expression. *Materials Science and Engineering C*, *98*(December 2018), 347–357. https://doi.org/10.1016/j.msec.2018.12.143

Salea, R., Widjojokusumo, E., Veriansyah, B., & Tjandrawinata Phd Ms Mba Frsc Frsph, R. (2014). Optimizing oil and xanthorrhizol extraction from Curcuma xanthorrhiza Roxb. rhizome by supercritical carbon dioxide. *Journal of Food Science and Technology*, *51*, 2197–2203. https://doi.org/10.1007/s13197-014-1272-3

Senanayake, D., Yapa, P., Dabare, S., Munaweera, I., Weerasekera, M., Etampawala, T., Sethunga, M., Attygalle, D., & Amarasinghe, S. (2025). Combined antimicrobial and anti-inflammatory properties of electrospun PCL nanohybrids infused with metal-turmeric oleoresin and metal-curcuminoids. *RSC Advances*, *15*, 20061–20083. https://doi.org/10.1039/d5ra01642h

Sleinus, D., Lovato, M. J., Platnieks, O., Sabalina, A., Gaidukovs, S., Franco, L., Puiggalí, J., & del Valle, L. J. (2025). Electrospun antimicrobial poly (lactic acid) foams with nanocellulose for enhanced hydrophilicity and controlled drug release. In *RSC Advances* (Vol. 15, Issue 9, pp. 6753–6763). https://doi.org/10.1039/d4ra08580a

Hashim, S. & Bakar, M., L. (2024). Antibacterial Activity of Turmeric (Curcuma longa) Extract Against *Staphylococcus aureus* and *Escherichia coli*. *Journal of Academia*, *12*(2), 195–200.

Tamayo, L., Santana, P., Forero, J. C., Leal, M., González, N., Díaz, M., Guiliani, N., Hamm, E., & Urzúa, M. (2022). Coaxial fibres of poly (styrene-co-maleic anhydride) @poly(vinyl alcohol) for wound dressing applications: Dual and sustained delivery of bioactive agents promoting fibroblast proliferation with reduced cell adherence. *International Journal of Pharmaceutics*, *611*, 121292. https://doi.org/10.1016/J.IJPHARM.2021.121292

Teanchai, K., Witit-anun, N., & Chaikhun, S. (2016). Characterization and Analyzation of Chitosan from Anadara granosa Shell. *Key Engineering Materials*, *675–676*, 463–466. https://doi.org/10.4028/www.scientific.net/KEM.675-676.463

Tolun, A., Sharifuzzaman, M., & Altintas, Z. (2025). Electrospun nanofibers of curcumin/HP-beta-CD/pullulan complex with enhanced solubility and controlled release in food and drug delivery

applications. *International Journal of Biological Macromolecules*, *300*, 140064. https://doi.org/10.1016/j.ijbiomac.2025.140064

Tsao, N., Chang, Y. C., Hsieh, S. Y., Li, T. C., Chiu, C. C., Yu, H. H., Hsu, T. C., & Kuo, C. F. (2021). AR-12 has a bactericidal activity and a synergistic effect with gentamicin against group a streptococcus. *International Journal of Molecular Sciences*, *22*(21). https://doi.org/10.3390/ijms222111617

Wang, T., Turhan, M., & Gunasekaran, S. (2004). Selected properties of pH-sensitive, biodegradable chitosan–poly (vinyl alcohol) hydrogel. *Polymer International*, *53*(7), 911–918. https://doi.org/10.1002/pi.1461

Wang, Y., Wang, X., Zhou, D., Xia, X., Zhou, H., Wang, Y., & Ke, H. (2023). Preparation and Characterization of Polycaprolactone (PCL) Antimicrobial Wound Dressing Loaded with Pomegranate Peel Extract. *ACS Omega*, *8*(23), 20323–20331. https://doi.org/10.1021/acsomega.2c08180

Wang, Y., Ying, T., Li, J., Xu, Y., Wang, R., Ke, Q., Shen, S., Xu, H., & Lin, K. (2020). Hierarchical micro/nanofibrous scaffolds incorporated with curcumin and zinc ion eutectic metal organic frameworks for enhanced diabetic wound healing via antioxidant and anti-inflammatory activities. *Chemical Engineering Journal*, *402*, 126273. https://doi.org/10.1016/j.cej.2020.126273

Warmasari, N. W. M., Ernawati, D. K., Indrayani, A. W., Dewi, N. W. S., & Jawi, I. M. (2020). Antibacterial Activity from Temulawak Extract (*Curcuma xanthorrhiza* Roxb) on Growth Inhibition of Staphylococcus epidermidis In Vitro. *Jurnal Epidemiologi Kesehatan Komunitas*, *5*(1), 1–7. https://doi.org/10.14710/jekk.v5i1.6909

Wenchao, L., Shi, L., Zhang, X., Liu, K., Ullah, I., & Cheng, P. (2017). Electrospinning of polycaprolactone nanofibres using H 2 O as benign additive in polycaprolactone/glacial acetic acid solution. *Journal of Applied Polymer Science*, *135*, 45578. https://doi.org/10.1002/app.45578

Xia, D., Liu, Y., Cao, W., Gao, J., Wang, D., Lin, M., Liang, C., Li, N., & Xu, R. (2022). Dual-Functional Nanofibrous Patches for Accelerating Wound Healing. *International Journal of Molecular Sciences*, *23*(18). https://doi.org/10.3390/ijms231810983

Yang, X., Li, L., Yang, D., Nie, J., & Ma, G. (2020). Electrospun Core–Shell Fibrous 2D Scaffold with Biocompatible Poly (Glycerol Sebacate) and Poly-l-Lactic Acid for Wound Healing. *Advanced Fibre Materials*, *2*(2), 105–117. https://doi.org/10.1007/s42765-020-00027-x

Yasmeen, S., Kabiraz, M., Saha, B., Qadir, Md., Gafur, Md., & Masum, S. (2016). Chromium (VI) Ions Removal from Tannery Effluent using Chitosan-Microcrystalline Cellulose Composite as Adsorbent. *International Research Journal of Pure and Applied Chemistry*, *10*(4), 1–14. https://doi.org/10.9734/IRJPAC/2016/23315

Yoshikawa, O., Basoli, V., Boschetto, F., Rondinella, A., Zhu, W., Thieringer, F. M., Xu, H., & Marin, E. (2025). Electrospun Polycaprolactone-Curcumin Scaffolds: Optimization of fibre production for enhanced Nanotopography and improved biological cell adhesion. *European Polymer Journal*, *222*(November 2024), 113616. https://doi.org/10.1016/j.eurpolymj.2024.113616

Yu, H., Chen, X., Cai, J., Ye, D., Wu, Y., & Liu, P. (2019). Dual controlled release nanomicelle-in-nanofibre system for long-term antibacterial medical dressings. *Journal of Biomaterials Science, Polymer Edition*, *30*(1), 64–76. https://doi.org/10.1080/09205063.2018.1549771

Zhang, H., Guo, M., Zhu, T., Xiong, H., & Zhu, L. M. (2022). A careob-like nanofibres with a sustained drug release profile for promoting skin wound repair and inhibiting hypertrophic scar. *Composites*

*Part B: Engineering*, *236*, 109790. https://doi.org/10.1016/J.COMPOSITESB.2022.109790

Zhao, J., Chen, L., Ma, A., Bai, X., Zeng, Y., Liu, D., Liu, B., Zhang, W., & Tang, S. (2024). Recent advances in coaxial electrospun nanofibres for wound healing. *Materials Today Bio*, *29*(September), 101309. https://doi.org/10.1016/j.mtbio.2024.101309